

Available online at www.sciencedirect.com**ScienceDirect**

Energy Procedia 69 (2015) 506 – 517

Energy
Procedia

International Conference on Concentrating Solar Power and Chemical Energy Systems,
SolarPACES 2014

Open volumetric air receiver based solar convective aluminum heat treatment furnace system

D.Patidar^a, S.Tiwari^a, P.K.Sharma^b, L.Chandra^{a,*}, R.Shekhar^b

a: Indian Institute of Technology Jodhpur, Old Residency Road, Jodhpur 342 011, India

b: Indian Institute of Technology Kanpur, Kalyanpur, Kanpur - 208 016, India

Abstract

The current heat treatment processes make use of electricity or fuel for generating heat. Solar energy is available in abundance in the states of Rajasthan and Gujarat in India. Annual global solar radiation of about $\geq 2400 \text{ kWh/m}^2$ is received in these regions. Use of the abundant solar thermal energy in heat treatment of metals would save energy and fuels. In view of this a concept of solar convective furnace system is described in this paper. As a starting point, heat treatment of aluminium is considered. For this system, requirements of industrial furnace are taken as basis. A scale-down retrofitted furnace is designed and analysed. The importance of different process stages like, solar thermal energy absorption, storage and utilization in design of such a system is presented. A thermodynamic analysis is performed to derive requirements for the achievement of a uniform heating at a pre-determined rate. Control strategy to meet the requirements is worked out. Air flow profile in the furnace is analyzed using CFD as a tool. Laser Doppler Velocimetry technique is used for measurement of velocity in a Plexiglas model of the scale-down furnace. Flow analysis using the adopted CFD tool shows non uniformities in air flow profile. To counter this, further modifications and improvements in the furnace structure are suggested. Evaluation of Open Volumetric Air Receiver (OVAR) using installed solar air tower simulation facility is also presented in the paper.

© 2015 The Authors. Published by Elsevier Ltd. This is an open access article under the CC BY-NC-ND license (<http://creativecommons.org/licenses/by-nc-nd/4.0/>).

Peer review by the scientific conference committee of SolarPACES 2014 under responsibility of PSE AG

Keywords: volumetric air receiver; convective furnace; solar energy; heliostat; CFD; LDV

* Corresponding author.

E-mail address: chandra@iitj.ac.in; dr.laltu.chandra@gmail.com

1. Introduction

Furnace is used for heat treatment or melting of material [1]. In conventional furnaces electrical heating is employed for such purpose [2]. The requirement of energy depends on the size and operating condition of a furnace [3]. Usually, the conversion efficiency of such a process is less than 30 % [3, 4]. It is expected that solar energy can be utilized for such purpose [5]. Such a system will avoid double conversion from fuel to heat and then from heat to electricity. Consequently, the efficiency should increase with saving of conventional fuel. Keeping this in view a concept of solar convective furnace is proposed and its schematic is shown in Figure 1. This Figure shows a solar thermal system integrated with a solar convective furnace, initially considered for heat treatment of aluminum, like, annealing. Aluminium annealing is carried out in a temperature range from 300 to 520°C [2] that requires 250 to 400 MJ/MT of thermal energy, even in India [6]. Concentrated Solar energy has been investigated for various applications including power generation, steel hardening [7, 8, 9].

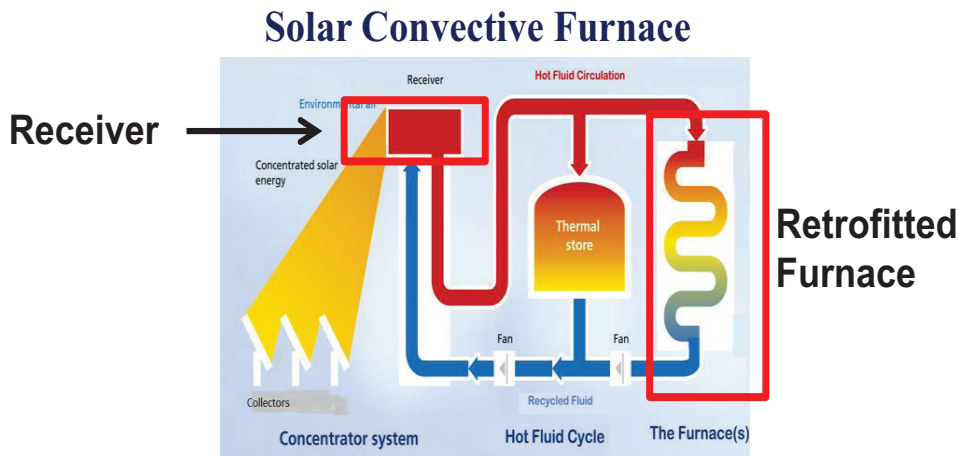


Figure 1: Schematic of concentrated solar thermal based retrofitted convective furnace

In the designed solar convective furnace system heliostat is used for collection and reflection of radiation to a receiver. The receiver is made of porous absorbers [5] and uses atmospheric air as heat transfer fluid. This receiver is termed as Open Volumetric Air Receiver (OVAR). The harnessed heat using OVAR results in increasing temperature of air. The obtained hot air will be utilized for annealing of aluminum to begin with. For this purpose, the existing annealing furnace is to be retrofitted. Retrofitting will ensure use of solar energy based heating in addition to the currently available electrical model of heating. Metal processing in a convective furnace requires uniform heating of metal ingots/ pieces. It also calls for maintaining the required rate of temperature rise. Therefore, detailed design and analysis of such a furnace concept is necessary for implementation. In view of the above, the following are presented in this paper:

- Concept and design of a retrofitted annealing furnace for aluminum
- Thermodynamic analysis and control strategy of the retrofitted furnace
- Evaluation of OVAR
- Flow measurement experiment and computational fluid dynamics (CFD) analysis of the retrofitted furnace

2. Solar convective aluminum heat treatment furnace system

Solar thermal energy absorption, storage and utilization are the major stages of the system as shown in Figure 1. The designed OVAR is shown in Figure 2a [5]. This comprises of porous cylindrical shaped absorbers and currently under investigation. For this purpose, an experimental solar air tower simulator (SATS) facility is installed at IIT Jodhpur as shown in Figure 2b [10]. This includes pebble bed thermal energy storage (TES) for providing the necessary control to the required amount of power during processing. A blower is used for suction and re-

distribution of the obtained hot air from the receiver. The following subsections provide an insight to the furnace design and its retrofitting.



Figure 2. (a) The designed circular porous absorber based OVAR; (b) SATS facility at IIT Jodhpur

2.1. Full Scale Annealing Furnace

An example of full scale industrial aluminum heat treatment furnace is shown in Figure 3a [11]. The dimensions of this furnace are presented in figure. The capacity of this furnace is about 500kW for processing of 16.4 m^3 of aluminum. This furnace comprises of a centrally located hearth having a porous grid at the bottom. The grid supports the metal ingots to be treated. Two number of side ducts are used for electrical heating of air.

Table 1. Details of full scale industrial aluminum heat treatment furnace

Dimension, m	Air temperature, °C	Ingot temperature, °C
Hearth: $3.5 \times 3.5 \times 3.5$	650	Initial: 100 ; Final: 600
Ingot: $3.2 \times 1.1 \times 0.48$		Time taken: 10.5 hrs

An air blower is used for generating the required air flow. The details of the furnace and its operating conditions are summarized in table 1. A layout of ingots placed on the supporting grid is shown in Figure 3b. For this layout resulting hydraulic diameter for the internal space between ingots is 0.31 m. The table also indicates the wide furnace temperature operating range from 100 to 600°C and the required time to achieve the same. This range also includes annealing temperature. In view of the aim of this paper the next sub-section presents a retrofitted solar convective furnace for annealing.

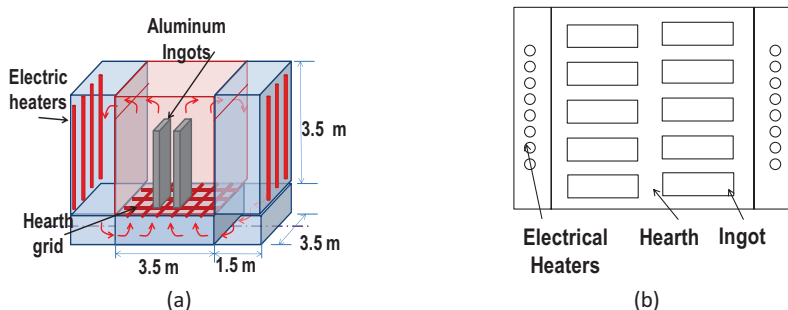


Figure 3. (a) Industrial Aluminum heat treatment furnace; (b) Typical layout of Aluminum ingots

2.2. Scale-down retrofitted solar convective furnace

A geometrically scaled down model of annealing furnace is shown in Figure 4a. A 1:15 scaled-down model of the presented furnace in previous sub-section. This results in capacity of 260W for processing. The dimensions length, width and height of retrofitted furnace and that of ingots are chosen accordingly. These are summarized in table 2.

Table 2. Dimensions of scaled-down furnace and the metal ingots

	Scale-down furnace hearth	Scale-down Ingot
Dimension, mm	235 x 235 x 235	213 x 73 x 32

The obtained hot air from OVAR is inducted via TES through two side ducts into furnace hearth. The employed divergent section is having an angle less than 10° [12]. This is to avoid reverse flow and to ensure flow uniformity at the inlet to side duct. This is shown in Figure 4a. The placement of metal ingots and their dimensions are given in Figure 4b. The hot air enters the hearth from bottom. Uniform air flow is essential for processing of all the metal ingots. Certain velocity or mass flow rate is required to achieve desired heat transfer rate. The relatively cooled air exits from the convergent hearth top and passes through TES driven by an air-blower. In view of expected, uniform processing of metal ingots, lump capacitive heating is assumed in the full scale furnace. From the available furnace operation parameters (t : heating time, T_∞ : Ambient air, T_i : Initial metal & T_f : Final metal temperature) convective heat transfer coefficient h is obtained using equation 1 [13]. In this equation ρ : density, V : Volume, A : surface area, c_p : specific heat capacity of metal ingot. Biot number (Bi) is then calculated for this h . The calculated value of $Bi < 0.1$ confirms that heating assumption is reasonable.

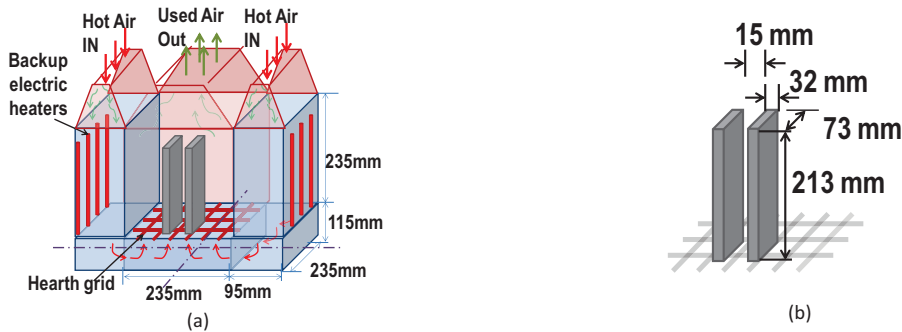


Figure 4. Schematic of (a) Retrofitted solar convective furnace; (b) Ingots placement in hearth

In the scaled-down model attempts are made to preserve at least the Bi in order to ensure uniform heating of the metal block. At the same time, it can be argued to conserve even the Fourier number (Fo) to attain the same processing time. However, for practical purpose it is difficult to ascertain both these parameters in the scaled-down model. In view of this, material of ingots is taken as stainless steel ($k=17 \text{ W/mK}$). The resulting value of h for scale down furnace compares well to that of full-scale furnace. In other words, flow regime is maintained. This is obtained by assuming internal flow between ingots. This indicates flow is in entry length regime. Using the obtained h and expression as in Eqn. (2) [14] the averaged Nusselt number (Nu) for a fully developed (fd) flow condition is obtained. This value is required for estimation of Reynolds number (Re) using Gnielinsky correlation as in Eqn. (3) [15]. This Re will provide the required mass flow rate of air.

Table 3. Scaling down parameters

Furnace	Parameter values
Full scale Furnace	$L_c = 0.24 \text{ m}$, $h=26$, $Bi=0.03$, $Fo=57.4$
Scale-down furnace	$L_c=0.015 \text{ m}$, $h=30.8$, $Bi=0.03$, $Re = 3400$, $f=0.038$

$$h = \frac{\rho V c_p}{t A_s} \ln \left(\frac{T_\infty - T_i}{T_\infty - T_f} \right) \quad (1)$$

$$\frac{\overline{Nu}_D}{\overline{Nu}_{D,fd}} = 1 + \frac{C}{(x/D)^m}, \text{ where } C = 1 \text{ \& } m = 2/3 \quad (2)$$

$$Nu_{fd} = \frac{(f/8)(Re-1000)Pr}{1+12.7(f/8)^{1/2}(Pr^{2/3}-1)}, \text{ valid for } 0.5 < Pr < 2000; 3000 < Re < 5 \times 10^6 \quad (3)$$

2.3. Thermodynamic analysis for control strategy

So far the design of full-scale and scaled-down model of heat treatment furnace is presented. The heating process must satisfy stringent requirements. This is to ensure quality of the processed material. In the designed solar convective furnace hot air is introduced via TES. Therefore, it is essential to devise a control strategy to ascertain the functioning of the designed furnace system. Such a process is featured by large inertia and time delays with time varying characteristics etc. The objective is to achieve the desired time varying heating profile or power input to the processed metal ingots. For this purpose a control strategy based on preliminary thermodynamic analysis is presented. For this analysis, the heating rate in terms of temperature 100 to 600°C in 10.5 hrs is conserved, see table 1. The assumptions for this analysis are (a) hearth is perfectly insulated (b) heat is transferred to metal blocks from surface (c) incompressible fluid flow with constant properties. The energy balance in hearth is as follows:

$$\text{Rate of heat loss by air (A)} = \text{Rate of heat transfer from air to metal (B)} = \text{Rate of heat gain by the metal (C)}. \text{With, } A = \dot{m}C_{pa}(T_i - T_o), B = h.A_s.(T_a - T_m) \text{ and } C = \rho.V.C_p.\left(\frac{dT_m}{dt}\right) \quad (4)$$

Here, \dot{m} = mass flow rate of the air (kg/sec); C_{pa} and C_{pm} = specific heat capacity of air and metal (kJ/kg-K); T_i and T_o = inlet and out air temperature in hearth; $T_a = \frac{T_i + T_o}{2}$; T_m = volume averaged metal temperature; h = heat transfer coefficient (W/m²-K); A_s = Surface area (m²); V = Volume of material (m³).

Boundary conditions: $T_i = 650^\circ\text{C}$; $\dot{m} = 5\text{gm/s}$ for the desired $h = 30\text{ W/m}^2\text{K}$ (see table 3)

Analytically solving the energy balance equations provide:

$$\text{Metal temperature} = T_m(t) = 650 - 550 \exp\left[\frac{-t}{\tau}\right] \quad (5)$$

$$\text{Air temperature at hearth outlet} = T_o(t) = 650 - 206.71 \exp\left[\frac{-t}{\tau}\right] \quad (6)$$

where constant $\tau = 1344.8\text{ sec}$

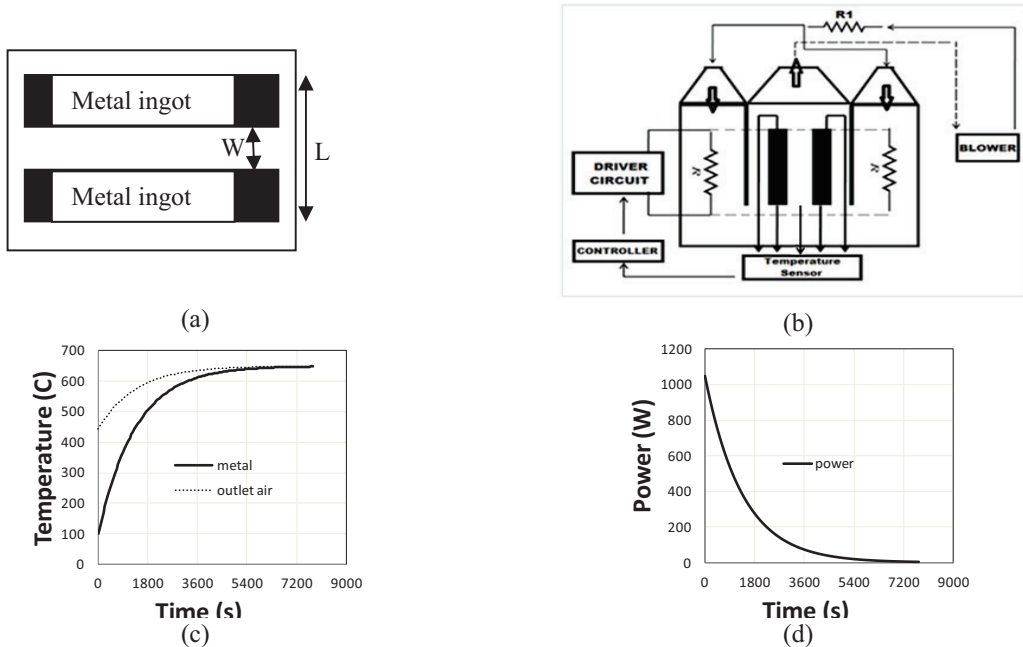


Figure 5. (a) Top view of an experimental furnace hearth with two metal ingots; (b) Experimental set-up for evaluating control strategy; Time dependent (c) temperature of metal and air in furnace and (d) Power requirement for processing of a single metal block

The resulting temperatures are shown in Figure 5c. In this analysis property of stainless steel is considered for material. This ensures Bi and h similarity with the full-scaled aluminum annealing furnace as in table 1. The schematic top-view of the planned experimental furnace with two metal ingots is shown in Figure 5a. The dimensions of these ingots are detailed in Table 4. These are placed at a distance of $w = 15\text{mm}$ with $L = 47\text{mm}$ as shown in Figure 5a.

Table 4. Dimensions of scaled-down furnace and the metal ingots

	Scale-down furnace hearth	Scale-down Ingot
Dimension, mm	200 x 62 x 200	200 (L) x 16 (B) x 200 (H)

This experiment will be used for evaluation of the designed control. The volume of one metal ingot in the 1:15 scaled-down furnace model is $\sim 64 * 10^{-5} \text{ m}^3$ with reference to metal volume of 16.37m^3 in full-scale model. For analysis a single metal block or ingot is considered. This is based on the symmetry in the hearth of furnace for the scaled-down model. As expected, in view of lower value of Fo the metal reaches the highest temperatures in about 2.5 hrs. Figure 5d shows that the power requirement will decrease with reduction in temperature between air and metal surface. The highest required power is about 1kW and its value decreases exponentially to zero in about 2.5 hours for the selected furnace with metal. The time averaged power requirement is about 180W during 2.5 hours. The controller should maintain this dynamic power requirement. The schematic of the planned controller is shown in Figure 5b. Air is made to pass over the heater R1 using a blower. The heat supplied to the air by R1 can be controlled by varying the power supply to R1. Thus the inlet air temperature (T_i) could be maintained at the desired value. The air carrying heat moves inside the furnace and loses its heat to the metal ingots placed on the hearth. The temperature sensor will offer information of the current state of temperature of the metal, inlet and outlet air. This information is sampled and converted to a digital signal by the ADC present in the Micro Controller Unit (MCU). Depending on the desired power to the metal and the power input from R1 the MCU will decide whether to switch the auxiliary Electrical heating(R) or not and also whether to increase or decrease the heat provided by heater R. This is done by generating a Pulse Width Modulated signal at one of the pins of MCU. The duty cycle of PWM signal is varied in accordance with the difference of desired power and power supplied by R1. The control action is given by the duty cycle values of the PWM signal which is applied to the switch operating the auxiliary heating (R).

3. CFD Approach

Computational Fluid Dynamics (FLUENT 13.0) has been used as a tool to analyze the air flow and heat transfer profile in the various sub-systems. The analysis of the convective furnace using CFD has been organized in three sections to develop the model: (i) Creation of mesh and applying the boundary conditions (ii) Mesh dependence study to identify optimum mesh element size, (iii) Use of selected mesh to generate flow profile along different lines, planes in the furnace. The generated CFD results are used to analyze the flow profile at different locations to identify regions of low or high flow which may affect the uniform heating of aluminum ingots in the furnace.

3.1. Geometry model and meshing

A 3-D geometry of 1:15 scale-down furnace is shown in fig. 6a. The modeled 1:4 of this scaled-down geometry, with two symmetry planes, for CFD analysis is shown in fig. 6b. The employed wall resolved polyhedral mesh with inflation is shown in Figure 6c and 6d. Uniform element sizes are ensured using sizing techniques of ANSYS. The different resolutions of the polyhedral meshes are presented in table 4. The considered aspect ratio is preserved.

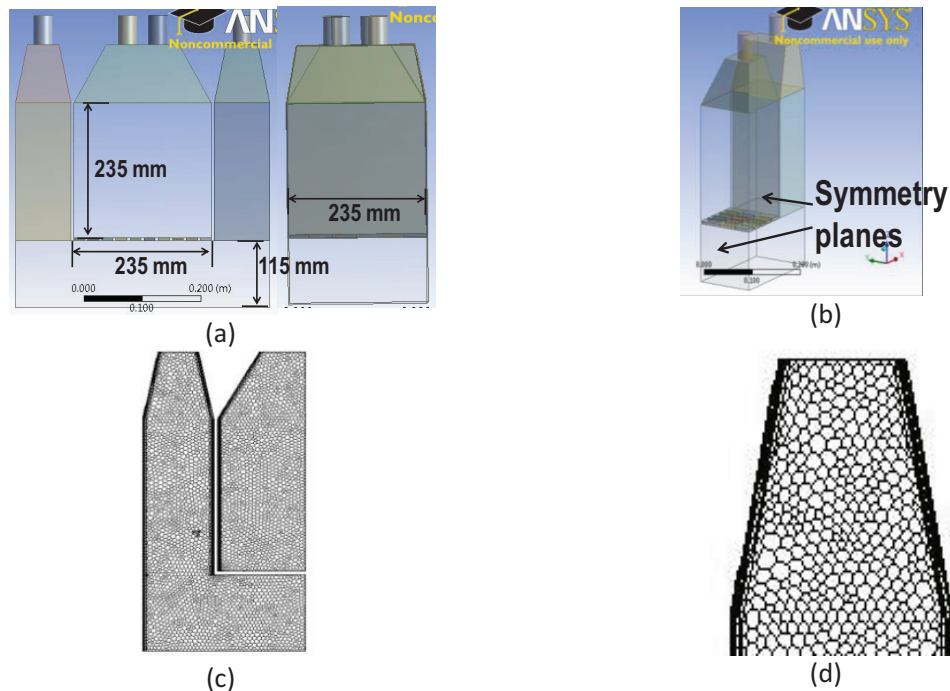


Figure 6. (a) Geometry of Scale down furnace; (b) 1/4th modeled geometry for CFD analysis with two symmetry boundaries (c) employed polyhedral elements in meshing; and (d) zoom in mesh elements near the inlet of side duct.

3.2. Numerical setup

For the CFD analysis Reynolds Averaged Navier Stokes equations are solved using specified polyhedral mesh with boundary layer. The numerical scheme for governing equations namely, continuity and momentum are detailed in table 5. The achieved convergence allows accepting the numerically analyzed results.

Table 5. Details of CFD set-up

Grid resolution	Max. aspect ratio	Equations	Flow Model & solution method	Spatial discretization	Convergence	y ⁺
9.6, 4.8 and 2.4 mm	44.7	Continuity and Momentum	- k-ε model - SIMPLE algorithm	1 st order upwind	10 ⁻⁵	3.75
Boundary conditions	At inlet: velocity= 10 m/s, gauge pressure=0 pascal; turbulent kinetic energy= 0.32 m ² /s ² ; turbulent dissipation rate=0.92 m ² /s ³ using inlet pipe diameter as length scale At outlet: gage pressure=0 pascal.					

3.3. Mesh dependence

Reducing the element size by half each time, three meshes are generated. The meshes with resolution, 9.6mm, 4.8mm and 2.4mm are termed as Mesh 1, Mesh 2 and Mesh 3, respectively. Analysis of velocity magnitude profile along line A-A as in furnace, shown in Figure 7b, for clarity is presented in Figure 7a. It is to be noted that 1/4th model geometry is used for CFD analysis. Figure 7a shows the computed velocity magnitude with three mesh resolution along line A-A from hearth wall to centre. In this figure X=0 denotes hearth wall. The CFD analyzed velocity magnitude profiles for the mesh 2 and 3 are practically the same. Hence, for safe side, mesh 3 is used for further flow analysis inside the furnace.

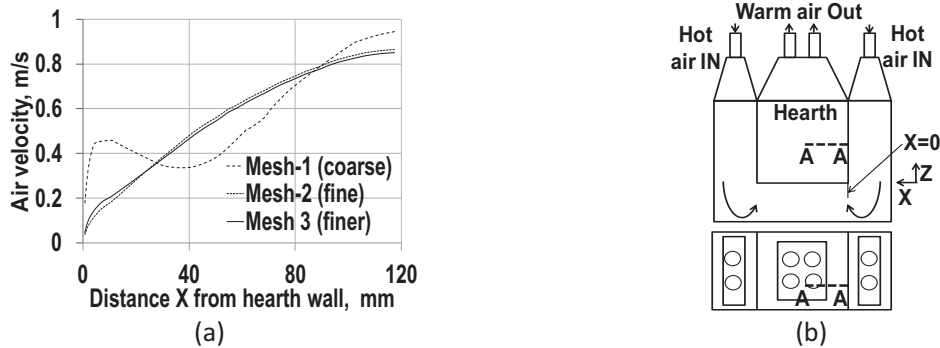


Figure 7. (a) Air velocity along A-A line in hearth region for mesh dependence analysis (b) schematic of scale down furnace showing A-A line

4. Experiment

4.1. Open Volumetric Air Receiver

The designed circular porous absorber based Open Volumetric Air Receiver (OVAR) is evaluated experimentally using the installed solar air tower simulator facility as shown in Figure 2. The detailed experimental and evaluation procedure is presented in [5]. This OVAR is heated electrically and it is shown that volumetric heating is achieved. Moreover, experiments have demonstrated that even partial heating of this receiver will allow achieving volumetric heating. The porosity of the designed receiver is 52% that compares well with Solair 200[16]. Such receivers are usually made of material with high thermal conductivity, like, Silicon-carbide ($\sim 100\text{--}300\text{ W/mK}$) in temperature range from $200\text{--}600^\circ\text{C}$ [17, 18, 19]. In the designed OVAR brass is used with comparable thermal conductivity for design evaluation only.

The organization of porous absorbers numbered 1-7 is shown in Figure 8a. Radiation after reflection from heliostat is concentrated onto these seven porous absorbers. Air is sucked in through the pores of these heated absorbers. As a result of temperature difference between air and absorber material, heat is transferred to air. An example of the measured temperature at the outlet of these absorbers is given in Figure 8b. In this experiment a power of 1500W is applied to the cylindrical surface of absorbers with a total mass flow rate (mfr) of air as 5gm/s . This results in an equivalent power to aperture (PoA)/mfr = 300 (kJ/kg) . The equivalent concentration onto the top surface of absorbers would be $\sim 400\text{ suns}$ ($1\text{sun} = 1\text{kW/m}^2$).

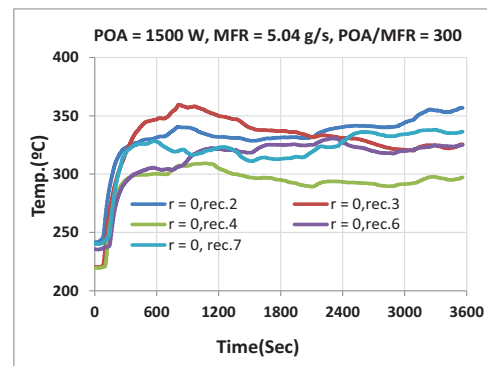
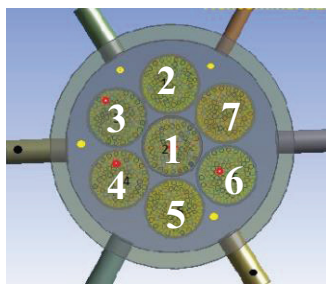


Figure 8. (a) Schematic of arrangement of seven circular porous absorbers and (b) The measured temperatures at the outlet of absorbers

The measured temperature at the outlet of absorbers for one hour duration is shown in Figure 8b. This clearly depicts achieving a quasi steady state with variation $< 3\%$ from the respective mean values. The average temperature is around $325\text{ }^{\circ}\text{C}$ for all the absorbers with overall non-uniformity $\sim \pm 25^{\circ}$ or 8% around this value. Hence, it can be inferred that the desired temperature can be achieved for the processing of material, like, aluminum. The estimated heat transfer effectiveness is about 65% .

4.2. Scale-down solar convective furnace model

Flow measurement experiments are conducted with the installed 1:15 scale-down Plexiglas furnace model as shown in Figure 9b. The schematic of the experimental set-up is shown in Figure 9a. An air blower of capacity $3.4\text{ m}^3/\text{min}$ is utilized to generate flow in the installed scale-down furnace. In the performed experiment, half of the furnace is blocked as shown in Figure 9c. This will allow achieving higher velocities with the considered flow rate. For measurement of velocity Laser Doppler Velocimeter (LDV) as shown in Figure 9d is utilized. The z and x-component of air velocity are measured. The measured values will allow validating the adopted CFD approach.

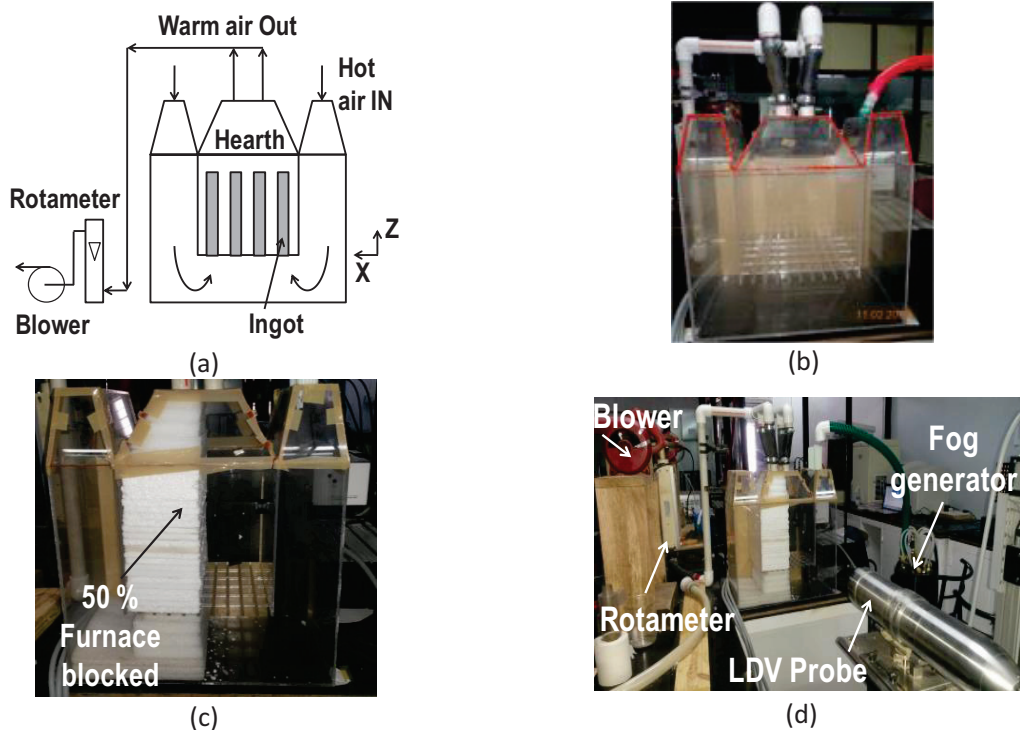


Figure 9. (a) Schematic of experimental setup; (b) Plexiglas model of scaled down furnace; (c) 50 % blocked furnace (d) Air velocity measurement using LDV

The specifications of the employed Laser Doppler Velocimeter (LDV) system are summarized in table 6. Pair of blue beams is used for measuring z-component of velocity. The frequency of one of the beams in each pair is shifted by 40 MHz using a Bragg cell. Similarly pair of green beams is used for x-component velocity measurements. Mineral oil droplets are used for seeding the flow.

Table 6. Specifications of Laser Doppler Velocimeter

Make & model	Light source	Fibre-optic probe, its focal length	Beam diameter, separation angle	Beams, fringe separation
TSI, FSA3500/4000	Argon Ion Laser (Coherent's Innova 70C)	TLN06-500, 363 mm	2.65 mm, 5.6°	Blue: 3.5513 μm Green: 3.7441 μm

For each measurement point 2000 samples were collected with a maximum record length in time of 120 s. Air velocity is measured using LDV along various lines in the furnace hearth and are presented in the next section.

5. Validation and CFD Analysis

In fig. 10a the measured values of x and z velocity components along the line H-H in the furnace, as shown in Figure 10b for clarity, are presented. As expected, high values are measured away from the walls. The negative values of z-velocity components indicate downward movement at the inlet region and even extend up-to about 130mm from the wall. The hearth wall is 95 mm from the furnace wall ($X=0$). Positive values of z-component of velocity beyond 130mm reveal the entry of air in the hearth region in the performed blocked furnace experiment. Consequently, the presence of a large vortex under the hearth region is inferred. The measured x-velocity components are much lower than that of z-velocity components along H-H line.

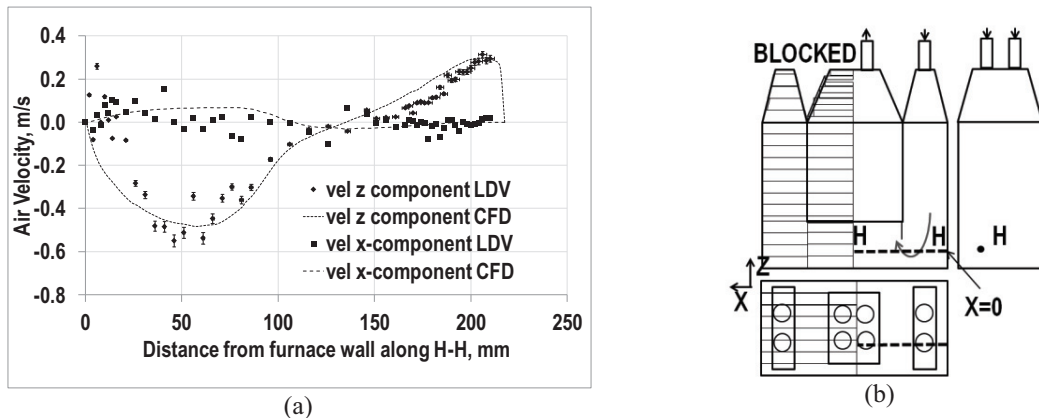


Figure 10. LDV experiment results (a) z & x velocity component in hearth of furnace (50% blocked) along line H-H; (b) Line H-H in bottom duct region

The CFD analyzed z-velocity component is plotted in Figure 10a for comparison with experimentally obtained values. This figure shows that the analyzed and experimental values compares fairly well in both negative and positive regions. Using wall resolved mesh, as expected, allows capturing velocity near the hearth wall at $X=0$ in duct region. In view of these observations, the adopted CFD approach is employed for evaluating flow in 1:4 furnace model with two symmetry boundaries, see Figure 6b. This simulates the real 1:15 scale-down model without blockage. The CFD analyzed z-velocity contour is shown in Figure 11a. The negative values indicate downward and positive values indicate upward movement of air. As expected, a large vortex under the hearth region is observed as shown in Figure 11b.

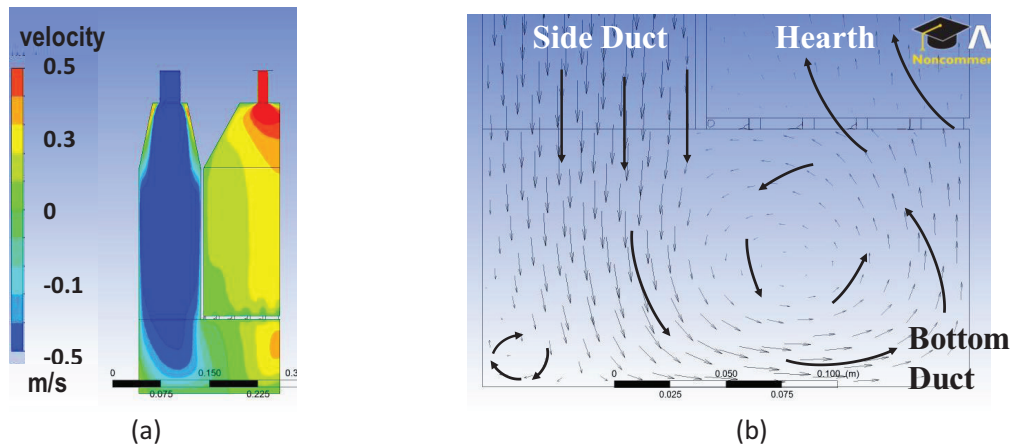


Figure 11. (a) Contour of x-velocity magnitude in CFD analyzed scale-down furnace model , (b) Velocity vectors under the hearth region

6. Conclusion and future work

The concept of a solar convective furnace system is presented. Utilization of solar thermal energy for annealing of aluminum would lead to increased efficiency of the furnace system. It would also mean reduction in fossil fuel usage. Design of a retrofitted scaled down convective furnace is presented. For the scale-down model Bi and Fr similarity is maintained using steel as metal ingot. Thermodynamic analysis for the scaled down retrofitted furnace is reported. The resulting time dependent profiles of metal and air temperature and also power requirement are presented. A control strategy to achieve the desired temperature profile of the metal is prescribed with a planned experimental set-up. Computational Fluid Dynamics (CFD) approach for flow analysis in the retrofitted scaled down furnace shows the presence of vortex under the hearth region of furnace. The approach is validated with the measured velocity profiles using Laser Doppler Velocimetry (LDV) technique. Future work aims to reduce or eliminate the formation of vortex by use of baffles, deflectors at suitable locations. This is essential to obtain uniform air velocity profile in hearth region for attaining uniform heating and therefore, processing, of metal ingot. Evaluation of OVAR has also been presented. Temperatures of 325°C have been attained at all the absorbers with a variation within 8%. The paper shows the feasibility of this concept in general.

Acknowledgement:

The authors duly acknowledge the received funding from Ministry of New and Renewable Energy, Govt. of India and support from Indian Institute of Technology. The authors convey special thanks to Prof. Deepak Fulwani for his input in framing the control strategy. Time-to-time support from project employees under MNRE/ECESTRE/20110007 is duly acknowledged.

References

- [1] Heat treating of aluminum and aluminum alloys, published Feb 2001, retrieved from <http://www.keytometals.com/Article139.htm> article
- [2] Rajan T.V., Sharma C.P., Sharma A: Heat Treatment: Principles and Techniques, chapter 16.1.
- [3] Aluminum; retrieved from <http://www.cseindia.org/userfiles/57-66%20Aluminium%281%29.pdf>
- [4] Bob Edwards and Vic Strauss, Electric Furnaces Complement Heat Treat Requirements for Gears, retrieved June 2 2013 from <http://www.gearsolutions.com>
- [5] Sharma, P., Sarma, R., Chandra, L., Shekhar, R., and Ghoshdastidar, P. S., Design and Evaluation of an Open Volumetric Air Receiver System for Heat Treatment of Aluminum, Under revision, Solar Energy Journal, 204.
- [6] Schumacher, Katja, Sathaye, Jayant, India's Aluminum Industry: Productivity, Energy Efficiency and Carbon Emissions; International Energy Studies; retrieved from <http://ies.lbl.gov/node/108>

- [7] Neumann, A., Groer, U, Experimenting with concentrated sunlight using the DLR solar furnace, *Solar Energy* Vol. 58, No. 4-6, pp. 181-190, 1996.
- [8] Rodriguez G.P., Damborenea J.J., Vazquez, A.J., Surface hardening of steel in a solar furnace, *Surface and coatings technology*, 92 (1997) 165-170.
- [9] Behar, Omer. Abdellah Khellaf, Kamal Mohammedi, A review of studies on central receiver solar thermal power plants, *Renewable and Sustainable Energy Reviews* 23 (2013) 12-39.
- [10] Sharma, P., Sarma R., Chandra, L., Shekhar, R., Ghoshdastidar, PS., On the design and evaluation of open volumetric air receiver for process heat applications. (Proc. SWC 2013), to appear in *Energy Procedia Journal*.
- [11] Personal interaction with Aaditya Birla Science and Technology Centre, Mumbai.
- [12] White Frank M., *Fluid Mechanics*, Chapter 6.11, Diffuser performance
- [13] Incropera, F.P., D.P. Dewitt, T.L. Bergman and A.S. Lavine, *Fundamentals of Heat and Mass Transfer*, Chap. 8, J. Wiley and sons, 2007.
- [14] Bhatti, M.S., and R.K. Shah, in S. Kakak, R.K. Shah, and W. Aung, Eds, *Handbook of Single Phase Convective Heat Transfer*, Chap. 4, Wiley-Interscience, New York 1987.
- [15] Gnielinski, V., *Int. Chem. Eng.*, **16**, 359, 1976.
- [16] Hoffschmidt B, et al., Performance evaluation of the 200-kWth HiTREC-II open volumetric air receiver. *Journal of Solar Energy Engineering* 2003; 125: 87–94.
- [17] Agrafiotis CC, et al., Evaluation of porous silicon carbide monolithic honeycombs as volumetric receivers/collectors of concentrated solar radiation. *Solar Energy Materials & Solar Cells* 2007; 91: 474–488.
- [18] Avila-Marin, Antonio L., Volumetric receivers in solar thermal power plants with central receiver system technology: A review. *Solar Energy* 2011; 85: 891–910.
- [19] Becker, M., Fend, T., Hoffschmidt, B., Pitz-Paal, R., Reutter, O., Stamatov, V., Steven, M., Trimis, D., Theoretical and numerical investigation of flow stability in porous materials applied as volumetric solar receivers. *Solar Energy* 2006, 80 (10): 1241–1248.